

AD-A059 301

LOCKHEED MISSILES AND SPACE CO INC PALO ALTO CALIF PA--ETC F/G 6/5
CORROSION PENETRATION IN CREVICES OF DENTAL AMALGAM.(U)

SEP 78 T KATAN, G RYGE

N00014-73-C-0397

UNCLASSIFIED

LMSC/D630101

NL

1 of 1

AD 50501



END
DATE
FILMED
12-78

DBC

UNCLASSIFIED

LEVEL

SECURITY CLASSIFICATION OF THIS PAGE (When Data Entered)

REPORT DOCUMENTATION PAGE

READ INSTRUCTIONS
BEFORE COMPLETING FORM

1. REPORT NUMBER Technical Report No. 6	2. GOVT ACCESSION NO.	3. RECIPIENT'S CATALOG NUMBER
4. TITLE (and Subtitle) CORROSION PENETRATION IN CREVICES OF DENTAL AMALGAM,	5. TYPE OF REPORT & PERIOD COVERED Interim Technical Report	6. PERFORMING ORG. REPORT NUMBER LMSC NO. D630101, 78-5
7. AUTHOR(s) T. Katan and G. Ryge	8. CONTRACT OR GRANT NUMBER(s) N00014-73-C-0397	9. PERFORMING ORGANIZATION NAME AND ADDRESS Lockheed Palo Alto Research Laboratory Materials Sciences Palo Alto, CA 94304
10. CONTROLLING OFFICE NAME AND ADDRESS Office of Naval Research 800 North Quincy Street Arlington, VA 22217	11. REPORT DATE September 1978	12. PROGRAM ELEMENT, PROJECT, TASK AREA & WORK UNIT NUMBERS
13. MONITORING AGENCY NAME & ADDRESS (if different from Controlling Office) Therodex/Katan (12) for Gunn/Ryge	14. NUMBER OF PAGES 23	15. SECURITY CLASS. (of this report) Unclassified
16. DISTRIBUTION STATEMENT (of this Report) Approved for Public Release; Distribution Unlimited.		
17. DISTRIBUTION STATEMENT (of the abstract entered in Block 20, if different from Report) SEP 27 1978		
18. SUPPLEMENTARY NOTES Prepared for publication in Journal of Electrochemical Society.		
19. KEY WORDS (Continue on reverse side if necessary and identify by block number) amalgam corrosion, crevice corrosion, dental amalgam.		
20. ABSTRACT (Continue on reverse side if necessary and identify by block number) A capillary-pore electrode with an optically transparent window for in situ viewing is used to screen three dental amalgams for their corrosion resistance. Results are in accord with more extensive clinical findings. Examinations by SEM and elemental microprobe show that a preferential corrosion of the poorly resistant tin-bearing phases involves dissolution of Sn with subsequent diffusion and deposition of an SnO hydrate preferentially on the gamma-one phase as a uniform, masking layer.		

AD A059301

DDC FILE COPY

DD FORM 1473

EDITION OF 1 NOV 65 IS OBSOLETE

UNCLASSIFIED

SECURITY CLASSIFICATION OF THIS PAGE (When Data Entered)

OFFICE OF NAVAL RESEARCH

Contract N00014-73-C-0397

TECHNICAL REPORT NO. 6

CORROSION PENETRATION IN CREVICES OF DENTAL AMALGAM

by

T. Katan and G. Ryge

Prepared for Publication

in the

Journal of the Electrochemical Society

Lockheed Palo Alto Research Laboratory
Lockheed Missiles & Space Company, Incorporated
A Subsidiary of Lockheed Corporation
Palo Alto, California 94304

September 7, 1978

Reproduction in whole or in part is permitted for
any purpose of the United States Government

Approved for Public Release; Distribution Unlimited

CORROSION PENETRATION IN CREVICES OF DENTAL AMALGAM

Theodore Katan*
Lockheed Palo Alto Research Laboratory
Palo Alto, California 94304

Gunnar Ryge
School of Dentistry, University of the Pacific
San Francisco, California 94115

ABSTRACT

An amalgam capillary-pore electrode with an optically transparent window for in situ viewing is used to screen three dental amalgams for their corrosion resistance. Results are in accord with more extensive clinical findings of decreased corrosion resistance in the order Dispersalloy > NTD > Microalloy. Subsequent examinations by SEM and elemental microprobe show that a preferential corrosion of the poorly resistant tin-bearing phases involves dissolution of Sn with subsequent diffusion and deposition of an SnO hydrate preferentially on the gamma-one phase as a uniform, masking layer.

INTRODUCTION

An intensification in research activity on the corrosion of dental amalgams by electrochemical methods has occurred only within the past 5 to 10 years and has done much to elucidate the

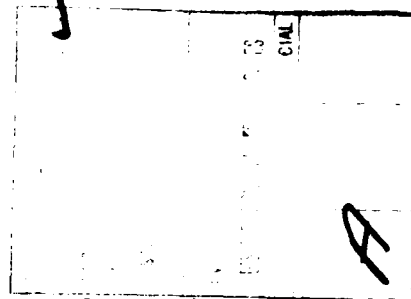
* Electrochemical Society Active Member.

Key words: amalgam corrosion, crevice corrosion, dental amalgam

principal steps involved in the corrosion process. Notably, Sarkar and Greener (1,2) have detailed the electrochemistry of conventional dental amalgams, showing that the height of the current density peak in the active regime is related to the amount of gamma-two phase**, while Marek and Hochman (3-5) have examined governing reactions and indicated how elementary tin and copper appear to exert their independent potentials in determining regimes of active, passive, and transpassive behavior. The new dispersion alloys have also received considerable attention (4-10).

Assuming that marginal breakdown is hastened by the onset of electrochemical corrosion at the crevice between amalgam and tooth, Marek and Hochman (5, 11) conducted experiments within small crevices and determined that significant reduction in pH and increase in chloride ion concentration can occur within the crevice during the progress of corrosion. Oxygen depletion and acidification within crevices are known to enhance corrosion (12, 13). These observations suggest that more detailed examinations are needed into the modes of dental crevice corrosion, in order that the corrosion penetration depth and reaction intensity profile within the crevice may be more specifically related to transport, kinetic, and geometrical parameters.

** Sarkar and Greener present a comprehensive discussion describing amalgamation and metallic phases in dental restorations (2).



In this study various dental alloys were placed in a well-characterized, known geometry of a capillary pore or crevice with an optically transparent window and then subjected to electrochemically induced corrosion at one end. This method was previously pioneered by others (11, 14, 15) and is modified here to observe the effects of several electrolytes with one specimen. The progress of corrosion was observed in situ by optical microscopy, and afterwards by scanning electron microscopy (SEM) and with elemental microprobe analyses. The current and overpotential usually diminish rapidly at some distance from the mouth of the pore so that the gradation in morphological manifestations along the pore could be examined and correlated with the extent and mode of the corrosion. During the optical microscopy, the coulombic input was pulsed so that the corrosion process could be stopped at any time to more accurately identify phases in their sequential involvement.

MATHEMATICAL CHARACTERIZATION

DeLevie (16) and others (17, 18) have indicated how the penetration depth of electrochemical reaction, L , in a pore or crevice can be approximately related to the crevice's cross sectional area, c , and perimeter, p , in terms of electrolyte resistivity, ρ , exchange current density, i_0 , temperature, T , Faraday's constant, F , gas constant, R , and the number of exchanged electrons, n .

$$L = \left[\frac{RTc}{nF i_0 \rho p} \right]^{1/2} \quad (1)$$

The principal assumptions are 1. constancy of impedances within the pore and 2. negligible influence of capacitance effects. These assumptions are reasonable for a small time interval during electrochemical reaction (corrosion), although, in fact, impedances within the crevice do change, and more elaborate mathematical models, such as those of Bennion et al (19, 20) are needed for an accurate description of the system. The simplified expression Eq. (1), can nevertheless provide a useful guide in interpreting the progress of corrosion in a crevice of dental alloy in a manner indicated by Katan and Szpak (21). During the course of corrosion the changes in reaction penetration depth would depend on the changes in a transport parameter, ρ , a kinetic parameter, i_0 , and in the geometrical configuration of the crevice, c and p .

EXPERIMENTAL DESCRIPTION

The apparatus consisted of a reaction cell, a stand for mounting and electrical contact of the electrodes, a zoom microscope* with a calibrated reticule placed above the cell, a potentiostat/galvanostat**, electronic programmer***, and an Ag/AgCl reference electrode probe.

The reaction cell had two rectangular amalgam specimens embedded 0.2 cm apart in an epoxy mount, Fig. 1. After the specimens were metallographically polished to a submicron finish with MgO in ethylene glycol, they were washed with triply distilled water and air dried at room temperature. Teflon tape****, 0.0060 cm thick, which previously had six 0.08 cm wide slots cut out to form the capillaries, was then placed on the specimens.

After mounting the cell on a stand to achieve stability and electrical contact from below the electrodes, a preselected electrolyte was placed in one of the slots formed by the Teflon tape, and a cover slide placed over the slot to enclose it as a capillary pore of known dimensions. Pore width and length were measured with

* Bausch & Lomb Stereozoom 7

** PAR Model 173

*** PAR Model 175

**** Temp-R-Tape, The Connecticut Hard Rubber Co., New Haven, Conn.

the calibrated reticule attachment of the microscope. After the passage of a preselected current at a preselected time interval, the surface of the anodic specimen was examined at 10 to 100 x and the extent of penetration of visible reaction product was measured. This procedure was repeated until the reaction front exhibited by visible corrosion product had developed well within the pore.

After concluding experiments with one slot, the cover slide was removed, and the slot was carefully dried with tissue. Then, another slot was filled with another electrolyte and the sequence of testing repeated. When the group of five solutions was tested with one amalgam, the Teflon tape was removed, the specimen washed in triply distilled water, air dried, and then prepared for SEM* analyses.

RESULTS AND DISCUSSION

Screening dental alloys.--In Table I the penetration depths are given for J & J Dispersalloy, SSW New True Dentalloy, and Caulk's Microalloy, with five electrolytes, 0.010, 0.10, and 1.0 N NaCl, as well as Ringer's solution and saliva. These data resulted from a current flow of 0.05 mA in 10 and 20 second increments, until a total charge of 5 mC was reached.

* Mark II

In all electrolytes, Dispersalloy exhibits less penetration than New True Dentalloy which, in turn, exhibits less penetration depth than Microalloy. These observations corroborate the general clinical findings of decreased visible corrosion in the same respective order (22). The relative severity of induced corrosion for the three alloys corresponds to these same alloys' clinical performance, Dispersalloy showing better marginal integrity and less corrosion over time than the conventional alloys. It is suggested on the basis of these findings that dental alloys may be generally screened by this method of observations of penetration depths.

Penetration depth is found to be increased for NaCl electrolyte as the concentration is increased, and thus as the resistivity, ρ , decreases, in qualitative accord with the mathematical model Eq. (1) and Table I. The penetration does not change with small changes in external current for a given charge, also in keeping with the premises of Eq. (1). Thus, variation in current from 0.050 mA to 0.50 mA, with the total passage of 5.0 mC, did not change penetration depths in Dispersalloy or NTD with 0.10 NaCl in the crevice space. With Microalloy, visible corrosion extended throughout the pore under the same conditions so that penetration depths could not be compared.

Penetration depths generally increased with increase in corrosion time until the entire crevice was coated with reaction product. Typically, corrosion products were visible at low magnification, up to 100 X, forming a darker zone near the cathode. For Microalloy, the very first application of current resulted in total penetration across the specimen along the crevice with a thin white film, as indicated by the "larger than 0.6 cm" notation, Table I. As subsequent charges were applied, there was an increase in thickness of the corrosion product on Microalloy.

Corrosion mode.--For Dispersalloy and New True Dentalloy, there was a distinct gradation in corrosion activity along each crevice or capillary space. At the edge of the specimen nearest to the cathode a dark area appeared early and extended into the crevice as additional pulses were applied. Ahead of the dark area, a light zone penetrated and was measured, resulting in the penetration depths of Table I. Based upon previous work (23) it was anticipated that surface regions of the specimens in the recesses of the pore that were just beginning to undergo corrosion would give the most meaningful clues to the corrosion mode, i.e., where product had not yet masked the surface and where current densities are relatively low. The polarization and local transfer current density normally decrease rapidly with penetration distance into a capillary pore, and the inceptions of

morphological manifestations are most readily observed afterwards in the recesses of the pore. Figs. 2 through 5 illustrate this. In Fig. 2 is given a SEM photograph of NTD in a heavily corroded section (near the cathode) at 500 and 2000 X. Similarly, in Fig. 3 the surface of Dispersalloy in the heavily corroded section is shown at 500 and 2000 X for one of the dispersed phases. In these pictures, taken within 0.01 cm of the pore mouth, the corrosion products are so abundant that the original surface is masked, and it is difficult to establish sequential steps resulting in the morphological changes.

In the remote end of the crevice or capillary pore it is easier to establish transport modes and processes that occur during the induced corrosion. Fig. 4a shows a 500 X magnification of Dispersalloy, and it is clear that corrosion is initiated in the Cu_6Sn_5 zone which was previously formed around the dispersed eutectic Ag-Cu spheres during amalgamation as previously observed (5). At the higher magnification, Fig. 4b, a depression appears along the edge of this particle indicative of dissolution of the Cu_6Sn_5 phase with diffusion of reaction product in the electrolyte, deposition of a film initiated on the gamma-one phase, and the development of some nodular deposits on the eutectic Ag-Cu phase in the center of the sectioned spherical particles. Deposition from bulk solution is

indicated by the nodular form of the deposit on the Ag-Cu eutectic phase and by overhang of the deposited film on the gamma-one phase at the edges of voids and etch pits, Fig. 4. The deposited film is estimated to be about 1500 A thick in Figs. 4 and 5 and to be relatively uniform in thickness, indicative of a diffusion step which is rapid compared to the dissolution and deposition steps.

For the conventional NTD alloy we see in Fig. 5 the typical (2) dissolution of the gamma-two phase, at 500 and 2000 X, with formation of reaction product as a thin layer on the gamma-one phase with overhang, and, also, with some evidence of nodular development on the original silver alloy particles, Ag_3Sn . The original silver alloy particles in both NTD and Dispersalloy appear to be initially free of reaction product, at least until a thick layer of product is formed, compare Figs. 2 and 3 with Figs. 4 and 5. Again, the mode of corrosion appears as a dissolution, followed by a rapid diffusion of dissolved species through the bulk electrolyte with preferred deposition of a uniform film on the gamma-one phase.

For both Dispersalloy and NTD the corrosive process appears to be accompanied by a dissolution of the most reactive phases, gamma-two on the conventional alloy and Cu_6Sn_5 on Dispersalloy, with deposition from solution of a thin, uniform reaction product on the gamma-one phase, Ag_3Hg_4 , and with lesser amounts on the relatively

inert gamma phase, Ag_3Sn , and Ag-Cu eutectic phase. As the induced corrosion proceeds, eventually even the gamma phases are covered with an adherent film of reaction product. At the frontal regions of the pore, where dissolution and deposition are more rapid than diffusion, the deposited layers are no longer uniform in thickness but the reaction product is preferentially developed around the dissolution sites in layers as thick as 5 microns, Figs. 2 and 3.

Elemental microprobe analyses of the reaction product showed Sn and O present as principal constituents in a variable atomic ratio approximately from 2.5:1 to 2:1, respectively, for both the conventional and dispersed alloys on the gamma-one Ag_2Hg_3 , and Cu-Ag phases, further substantiating the dissolution-diffusion-deposition mode of corrosion and indicating tin as the diffusing element. Deposition of reaction product as observed at the cathode, also corroborating the proposed reaction mode of dissolution-diffusion-deposition. From the atomic ratios and from potentiometric observations of Marek and Hochman (4) it is suggested that the reaction product contains SnII as an indefinite hydrate of SnO (24), possibly as $\text{SnO} \cdot x\text{H}_2\text{O}$ with $1 \leq x \leq 1.5$. Other workers have found SnO as a principal reaction product (25). with more extensive corrosion for longer time spans there is evidence for SnO_2 formation (26).

If formation of tarnish is necessary to protect dental alloys, as has been suggested (10,25), then it appears that small amounts of the weakly corrosion-resistant gamma-two or Cu_6Sn_5 phases may actually be needed to serve this function, i.e., by acting as a source for the deseminated SnO layer (tarnish). The deposit may serve not only to protect the weak gamma-one phase by masking it with a protective film but also to reduce corrosion penetration into crevices by blocking the crevice space with the SnO deposit, eventually increasing the effective ρ in Eq. (1), and thereby improving marginal integrity. If the gamma-two and Cu_6Sn_5 phases are present only infrequently, so as not to form an interconnected phase or weaken the structure, then direct loss of structural integrity by their dissolution should be minimal while they serve this protective function.

CONCLUSIONS

A capillary-pore, amalgam electrode with an optically transparent window can be prepared for in situ microscopic viewing of penetration depth of visible reaction product. Comparisons of these penetration distances for three alloys in several electrolytes show a direct relation to the more extensive clinical observations of marginal integrity and indicate that capillary-pore electrodes may be more generally useful in screening new dental alloys.

Corrosion proceeds by dissolution of Sn from sites at the tin-rich phases, Cu_6Sn_5 in Dispersalloy and the gamma-two Sn_{7-8}Hg in NTD, by diffusion of an Sn II bearing species away from these dissolution sites, and by deposition preferentially on the gamma-one phase as a uniform film containing an SnO hydrate. Some deposition of particulate $\text{SnO} \cdot x\text{H}_2\text{O}$ also occurs on the Ag-Cu eutectic of Dispersalloy and the gamma phase, Ag_3Sn , of NTD as a less frequent mode of film formation at low current densities. Under normal conditions of slow corrosion, the diffusion step appears to be rapid compared to the deposition step.

Marginal integrity at amalgam restoration may be preserved by the protective SnO hydrate films preferentially masking the gamma-one phases which are more easily corroded than the Cu-Ag eutectic or Ag_3Sn phases, and by blocking of the crevices by SnO product between tooth and implant.

ACKNOWLEDGEMENTS

This study was supported by the Office of Naval Research and by the Pacific Dental Research Foundation.

This was Paper 102 presented at the Atlanta, Georgia Meeting of the Society, October 9-14, 1977.

REFERENCES

1. N.K. Sarkar and E.H. Greener, J. Dent. Res. 53, 925 (1974).
2. N.K. Sarkar and E.H. Greener, J. Oral Rehab. 2, 49 (1975).
3. M. Marek and R.F. Hochman, Abstr. No. 63, 50th IADR Meeting, 1972, Las Vegas.
4. M. Marek, R.F. Hochman, and M.F. Butler, Abstr. No. 194, 51st IADR Meeting, 1973, Washington.
5. M. Marek and R.F. Hochman, Abstr. No. 881, 54th IADR Meeting, 1976, Miami Beach.
6. K.D. Jorgensen, Int. Dent. J. 26, 369 (1976).
7. N.K. Sarkar and E.H. Greener, J. Dent. Res. 51, 1675 (1972).
8. E.H. Greener, J. Dent. Res. 55, 1142 (1976).
9. P.J. Staheli and J.A. von Fraunhofer, J. Dent. 1, 228 (1973).
10. R.W. Phillips, "Skinner's Science of Dental Materials," 7th Ed., W.B. Saunders Co., Philadelphia, (1973)
11. M. Marek and R.F. Hockman, Abstr. No. L-166, 53rd IADR Meeting, 1975, London.
12. U.R. Evans, "The Corrosion and Oxidation of Metals," Edward Arnold Ltd., London (1960).
13. I.L. Rosenfeld and I.K. Marshakov, Corrosion, 20, 115t (1964); Zh. Fiz.Khim., 30, 2724 (1956).
14. P. Reutschi, "Power Sources," vol. 4, p.381, Oriel Press, Brighton (1972).
15. E. McCafferty, J. Electrochem. Soc., 121, 1007 (1974).
16. R. De Levie in "Advances in Electrochemistry and Electro-analytical Engineering," P. Delahay, Editor, p. 336, Interscience Publishers, New York (1967).
17. C. Wagner, Plating 48, 997 (1961).
18. S. Szpak and T. Katan, Proc. Electrode Materials and Processes, vol. 77-6, The Electrochem. Soc., Princeton, p. 770 (1977)

19. J.S. Dunning, D.N. Bennion, and J. Newman, J. Electrochem. Soc. 118, 1251 (1971).
20. H. Gu, D.N. Bennion, and J. Newman *ibid*, 123, 1364 (1976).
21. T. Katan and S. Szpak, Electrochem. Soc, Ext. Abstr. 76-2, 59 (1976).
22. D.B. Mahler, L.G. Terkla, and J. Van Eysden, J. Dent. Res., 52, 823 (1973)
23. T. Katan, S. Szpak. and D.N. Bennion, J. Electrochem. Soc., 121, 757 (1974).
24. N.V. Sidgwick, "Chemical Elements and Their Compounds," Oxford University Press, London, p. 620 (1950).
25. B.S. Abadir, Corros. Sci. 17, 219 (1977).
26. E. Wagner, Deutsch. Zahnaerztl. Z. 17, 99 (1962).

Table I. Penetration of visible reaction product for three alloys*

Alloy	Penetration depth, cm				
	NaCl <u>0.01N</u>	NaCl <u>0.1N</u>	NaCl <u>N</u>	Ringer	Saliva
Dispersalloy	0.12	0.17	0.22	0.22	0.03
New True Dentalloy	0.14	0.27	0.33	>0.60	0.20
Microalloy	>0.60	>0.60	>0.60	>0.60	>0.60

*Crevice corrosion induced by 0.05 mA for 5 mC.
 Crevice dimensions: 0.6 cm x 0.08 cm x 0.006 cm.

FIGURES

Fig. 1. Arrangement of electrolyte cell showing placement of electrodes, electrical contact holes, and crevice spacing.

Fig. 2. Extensively corroded New True Dentalloy (NTD) near mouth of crevice opening. Mark represents 80 μm for a., and 20 μm for b.

Fig. 3. Extensively corroded Dispersalloy near mouth of crevice opening. Mark represents 80 μm for a., and 20 μm for b.

Fig 4. Dispersalloy in the recesses of the crevice at the inception of electrochemically induced corrosion. Numbered lines identify phases and materials present (2): 1. Ag-Cu eutectic phase present as spherical particles before amalgamation (setting), 2. Cu_6Sn_5 zone surrounding Ag-Cu eutectic phase and formed during amalgamation, 3. gamma phase, Ag_3Sn originally present before setting, 4. gamma-one phase, Ag_2Hg_3 , formed from Hg and Ag_3Sn during setting and now coated with reaction product, 5. nodular reaction product on eutectic Ag-Cu phase, 6. typical voids. Mark represents 80 μm for a., and 20 μm for b.

Fig. 5. New True Dentalloy in the recesses of the crevice at the inception of electrochemically induced corrosion. Numbered lines identify phases and materials present (2): 1. gamma phase, Ag_3Sn , originally present before amalgamation (setting), 2. void and reaction product left by gamma-two phase, Sn_{6-7}Hg , after undergoing dissolution by the induced corrosion (the gamma-two

phase is formed during setting from Hg and the gamma phase), 3. gamma-one phase, Ag_2Hg_3 , formed from Hg and Ag_3Sn during setting and now coated with product, 4. nodular reaction product on the gamma, Ag_3Sn , phase, 5. typical voids. Mark represents 80 μm for a., and 20 μm for b.

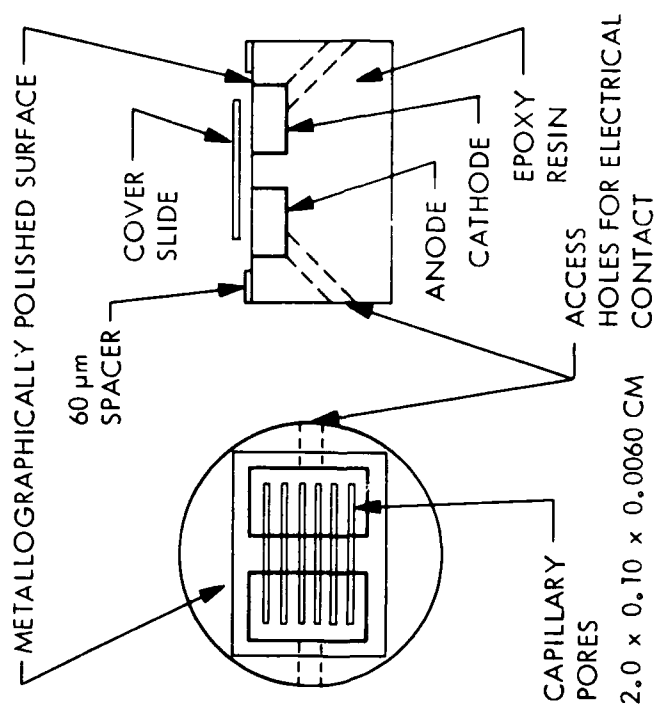


Fig. 1. Arrangement of electrolyte cell showing placement of electrodes, electrical contact holes, and crevice spacing.

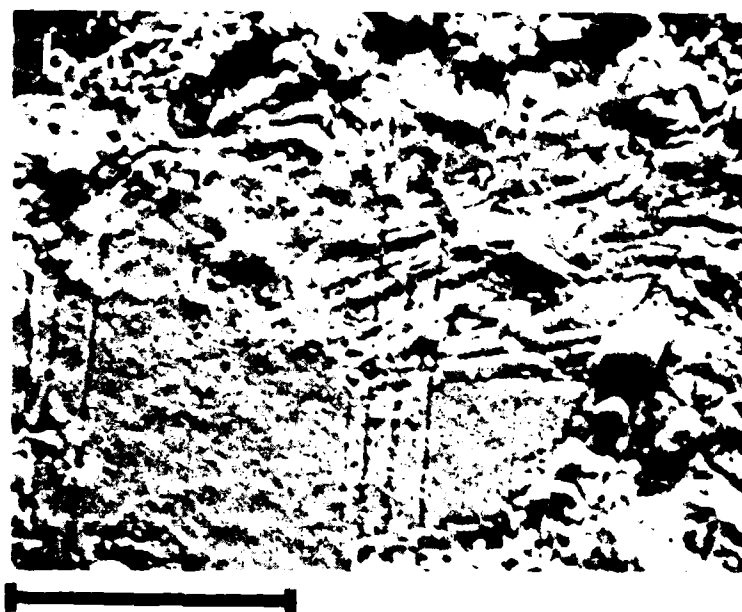
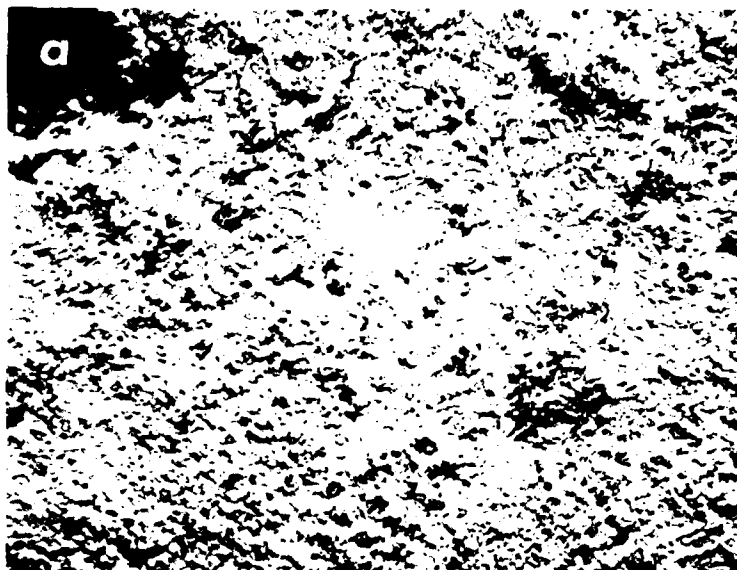


Fig. 2. Extensively corroded New True Dentalloy (NTD) near mouth of crevice opening. Mark represents $80\text{ }\mu\text{m}$ for a., and $20\text{ }\mu\text{m}$ for b.

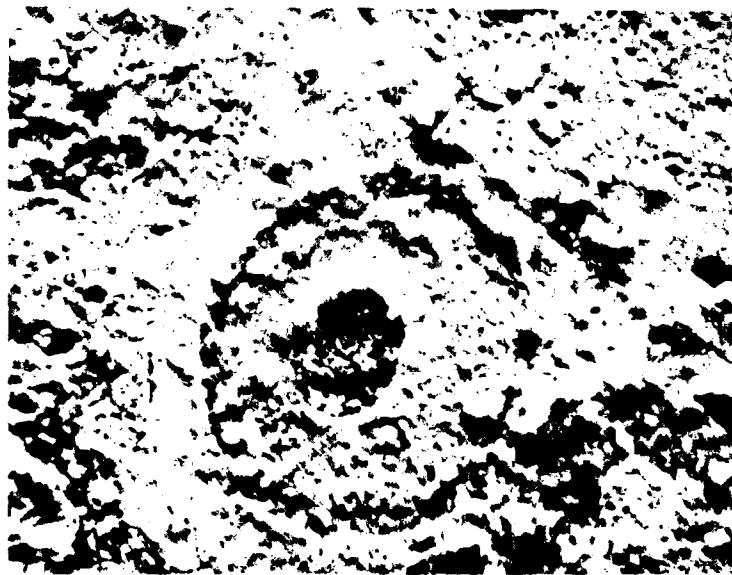
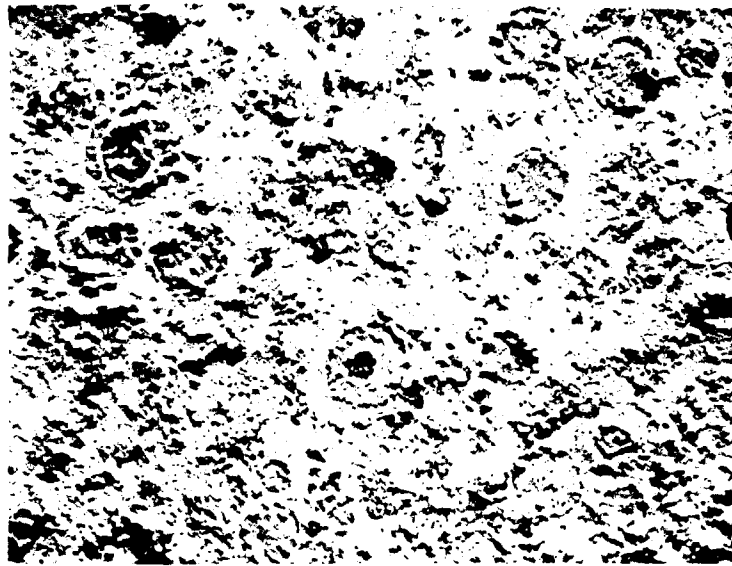


Fig. 3. Extensively corroded Dispersalloy near mouth of crevice opening. Mark represents 80 μm for a., and 20 μm for b.

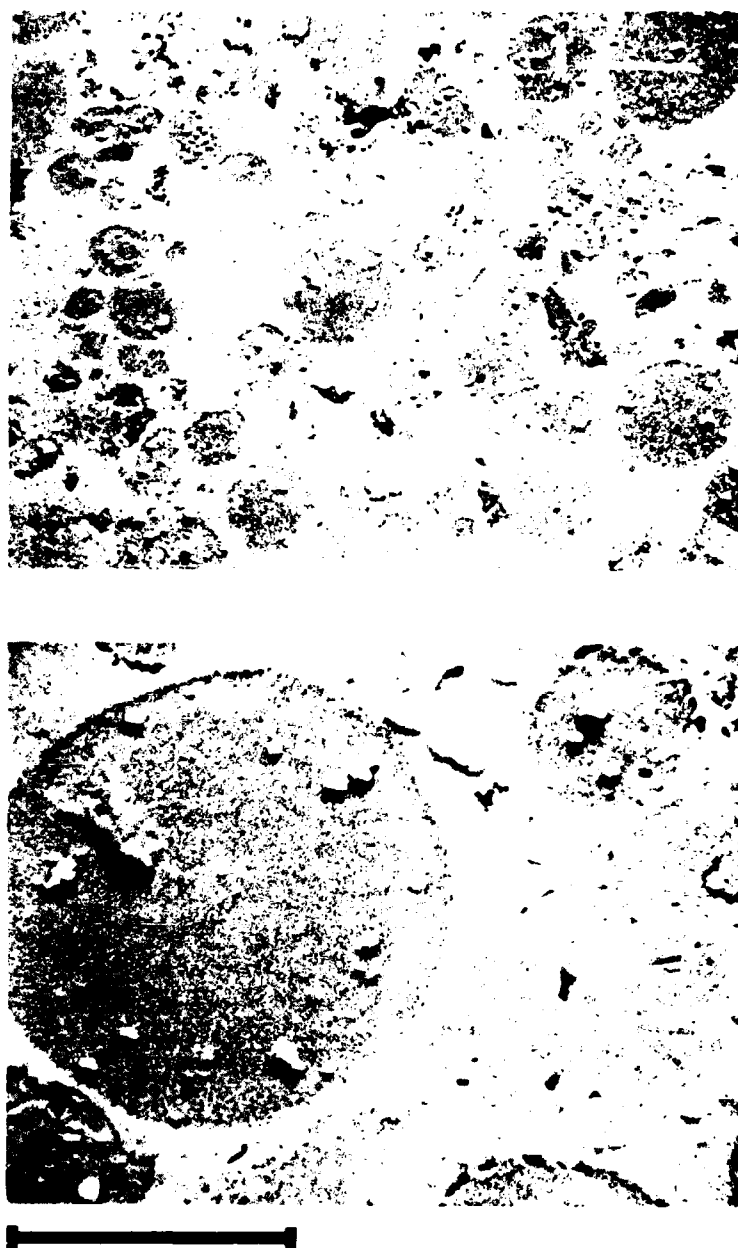


Fig. 4. Dispersalloy in the recesses of the crevice at the inception of electrochemically induced corrosion. Numbered lines identify phases and materials present (2): 1. Ag-Cu eutectic phase presents as spherical particles before amalgamation (setting), 2. Cu_6Sn_5 zone surrounding Ag-Cu eutectic phase and formed during amalgamation, 3. gamma phase, Ag_3Sn originally present before setting, 4. gamma-one phase, Ag_2Hg_3 , formed from Hg and Ag_3Sn during setting and now coated with reaction product, 5. nodular reaction product on eutectic Ag-Cu phase, 6. typical voids. Mark represents $80 \mu\text{m}$ for a., and $20 \mu\text{m}$ for b.

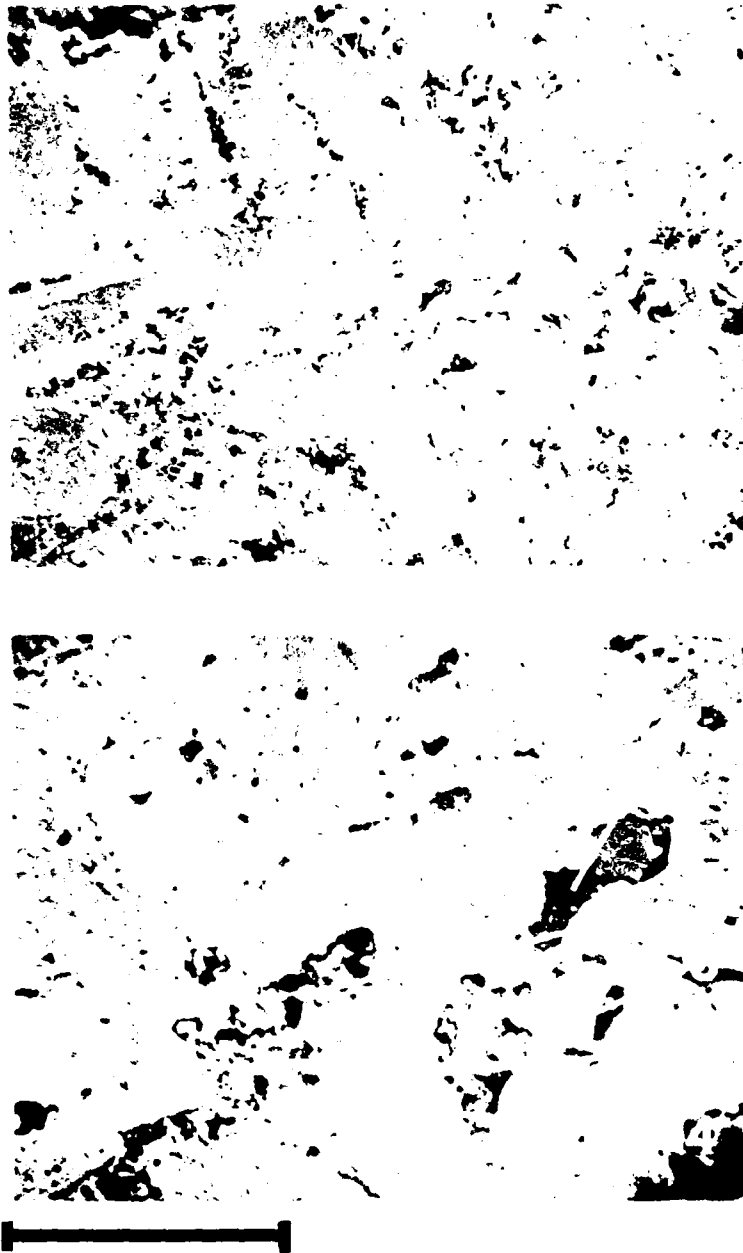


Fig. 5. New True Dentalloy in the recesses of the crevice at the inception of electrochemically induced corrosion. Numbered lines identify phases and materials present (2): 1. gamma phase, Ag_3Sn , originally present before amalgamation (setting), 2. void and reaction product left by gamma-two phase, Sn_{6-7}Hg , after undergoing dissolution by the induced corrosion (the gamma-two phase is formed during setting from Hg and the gamma phase), 3. gamma-one phase, Ag_2Hg_3 , formed from Hg and Ag_3Sn during setting and now coated with product, 4. nodular reaction product on the gamma, Ag_3Sn , phase, 5. typical voids. Mark represents 80 μm for a., and 20 μm for b.